PERSPECTIVE

Phenomenology of quantum turbulence in superfluid helium

Ladislav Skrbek[a,1], David Schmoranzer[a], Šimon Midlik[a], and Katepalli R. Sreenivasan[b,1]

Edited by David A. Weitz, Harvard University, Cambridge, MA, and approved February 22, 2021 (received for review December 4, 2020)

Quantum turbulence—the stochastic motion of quantum fluids such as ^{4}He and ^{3}He-B, which display pure superfluidity at zero temperature and two-fluid behavior at finite but low temperatures—has been a subject of intense experimental, theoretical, and numerical studies over the last half a century. Yet, there does not exist a satisfactory phenomenological framework that captures the rich variety of experimental observations, physical properties, and characteristic features, at the same level of detail as incompressible turbulence in conventional viscous fluids. Here we present such a phenomenology that captures in simple terms many known features and regimes of quantum turbulence, in both the limit of zero temperature and the temperature range of two-fluid behavior.

quantum turbulence | pure superfluid state | two-fluid state | Vinen and Kolmogorov turbulence

Turbulence is ubiquitous in Nature. Although it is an unfinished problem in science, incompressible turbulence in classical viscous fluids described by the Navier–Stokes equations, especially its decay without sustained production, as in the case of homogeneous and isotropic turbulence (HIT), is understood sufficiently well at the phenomenological level. Its properties can be described in surprisingly tangible detail (1). Quantum turbulence (QT) (2, 3) occurs in quantum fluids displaying superfluidity and two-fluid behavior at finite temperatures, such as the liquid phase of ^{4}He below the lambda temperature T_λ or the superfluid B phase of ^{3}He (4). Physical properties of quantum fluids cannot be described entirely by classical physics contained in the Navier–Stokes equations. Most physical properties of He II and ^{3}He-B are understood within the phenomenological two-fluid model, with the following main features. For temperatures $T < T_\lambda \approx 2.2$ K, liquid ^{4}He, called He II, is described as if it is composed of two interpenetrating constituents, the superfluid of density ρ_s and the normal fluid of density ρ_n; for ^{3}He-B the corresponding temperature $T_c \approx (1-3)$ mK, depending on the pressure. The viscous normal fluid consists of a gas of thermal excitations and carries the entire entropy content of the liquid. At relatively "high" temperatures (approximately above 1 K in He II and >200 μK in ^{3}He-B), the mean-free path is small and the thermal excitations can be described hydrodynamically as a fluid with finite viscosity. It coexists with the inviscid superfluid component carrying no entropy. The total density ρ of the liquid is nearly temperature independent and satisfies $\rho = \rho_n + \rho_s$. In the $T \to 0$ limit, helium is entirely a superfluid ($\rho_s/\rho \to 1$ and $\rho_n/\rho \to 0$), while superfluidity vanishes at the high temperatures just stated ($\rho_s/\rho \to 0$ and $\rho_n/\rho \to 1$).

Under isothermal conditions, the two fluids move independently when flow velocities are small. When a certain critical velocity is exceeded, however, thin vortex lines are formed in the superfluid component. Their circulation is not arbitrary as in classical fluids but quantized (5, 6) in units of $\kappa = h/M$ (usually singly), where h is Planck's constant and M is the mass of the superfluid particle (in the He II which is bosonic, $M = m_4$, the mass of the ^{4}He atom, while in the fermionic ^{3}He-B $M = 2m_3$, mass of the Cooper pair, twice the mass of the ^{3}He atom). The interaction of these quantized vortices gives rise to a tangle of quantized vortices, whose dynamics are QT's essential ingredient.

In the experimentally challenging limit of zero temperature with no normal fluid, QT consists only of the dynamical and disordered tangle of quantized vortex lines and can be called pure superfluid turbulence. The quantity characterizing the intensity of superfluid turbulence is the vortex line density, L,

[a]Faculty of Mathematics and Physics, Charles University, 121 16 Prague, Czech Republic; and [b]Department of Physics, Courant Institute of Mathematical Sciences, Tandon School of Engineering, New York University, New York, NY 11201

Author contributions: L.S. and D.S. designed research; D.S. and Š.M. performed research; D.S. and Š.M. analyzed data; and L.S. and K.R.S. wrote the paper.

The authors declare no competing interest.

This article is a PNAS Direct Submission.

[1]To whom correspondence may be addressed. Email: Ladislav.Skrbek@mff.cuni.cz or katepalli.sreenivasan@nyu.edu.

Published March 31, 2021.

which is the length of vortex line per unit volume. There exist two distinctly different and well-defined turbulent regimes called the Vinen (or ultraquantum) turbulence and the Kolmogorov (or quasiclassical) turbulence, the latter having various analogies with that in classical fluids.

At finite temperatures with the two-fluid behavior, QT may or may not involve turbulent motion of the normal fluid. When vortex lines are present in the isothermal flow, the otherwise independent normal and superfluid velocity fields become coupled by mutual friction acting at all relevant length scales, adding more complexity. Still, Vinen and Kolmogorov forms of quantum turbulence exist. We shall discuss them when the normal and superfluids flow counter to each other (called counterflow), for which there is no obvious classical analogue, and when they flow in parallel (coflow).

In this article we offer a systematic phenomenological description of various forms of QT in helium superfluids and compare them with turbulence of viscous fluids. For simplicity, our analysis is focused on three-dimensional (3D) HIT and based on experimental observations but, toward the end, employs models that treat the superfluid component containing the vortex tangle as a continuum possessing an effective "superfluid viscosity." The reason is that, even though the essential information in QT lies at small scales between vortex lines, their coarse graining enables useful views of the continuum type to be valid.

Pure Superfluid Turbulence

We start with the zero-temperature limit. In the frame of the two-fluid model both He II and ^{3}He-B are purely superfluid. As in classical turbulence, we have to consider only one velocity field. However, this velocity field is subject to the quantum mechanical constraint that the vorticity is zero everywhere except within the cores of quantized vortices.

The Model. In classical HIT, the finite size D of the turbulent box bounds the largest scale. The turbulent energy is supplied at some characteristic scale $M \le D$, which might be the size of a bluff body, the mesh size of the turbulence-generating grid, or D itself. In a steady state, the turbulent kinetic energy, K, and the rate of energy dissipation ε at small scales are related by $\varepsilon = -dK/dt$. Nonlinearity ensures that the energy is dissipated in a different range of scales than the injection range. By the processes of advection and stretching, the energy is thought to undergo the Richardson cascade down the scales until it reaches small scales of dissipation. The characteristic scale around which the turbulent energy eventually dissipates is the Kolmogorov scale $\eta \equiv (\nu^3/\varepsilon)^{1/4}$, where ν is the fluid viscosity; the corresponding Kolmogorov wavenumber $k_\eta = 2\pi/\eta$. One can also define, taking ν and ε as the only relevant variables, a corresponding velocity scale $u \equiv (\nu\varepsilon)^{1/4}$, which characterizes the motion of the scale η; the characteristic Reynolds number $\mathrm{Re}_\eta = u\eta/\nu \equiv 1$. From these considerations, scales smaller than η are not relevant to turbulence dynamics in a classical viscous fluid.

If the energy input at scale M is small enough for the Kolmogorov dissipation length η to be of the order of M, no turbulence can be created. Upon increasing ε, η becomes smaller and crosses M; gradually an "inertial range" of scales develops between M and η. According to our present understanding, the part of the spectrum for $k < M$ acquires a k^2 slope by the equipartition theorem, in agreement with the Birkhoff–Saffman invariant (7, 8). By requiring the spectral energy density $E(k)$ in the inertial range to depend only on the wavenumber k and ε (which is transmitted across the inertial range without dissipation), one arrives at the celebrated Kolmogorov form $E(k) = C\varepsilon^{2/3}k^{-5/3}$, where the constant C is experimentally known to be about 1.62 ± 0.17 (9).

After the cessation of energy input, the energy-containing scale grows with time and could saturate at D at some point. Although η also grows with time, leading to a shorter inertial range, considerable scale separation could persist and the spectrum in the decaying state could retain the same form as above. In this state of decay (10), it is possible to solve for the energy as a function of time. The result is that $\varepsilon \propto t^{-2}$ and the turbulent energy decays as $K \propto t^{-2}$.

In pure superfluid turbulence, there is no viscosity and hence no dissipative scale η. The flow exists down to the smallest scale, which is the size of the vortex core $\xi_4 \approx 0.1$ nm in He II and $\xi_3 \approx 10$ to 60 nm in ^{3}He-B. One can, however, define the superfluid Reynolds number Re_Q by replacing the kinematic viscosity ν by the quantum of circulation κ of the same dimensions, and ask for the length scale ℓ_Q at which $\mathrm{Re}_Q = u_Q\ell_Q/\kappa \equiv 1$, where $u_Q \equiv (\kappa\varepsilon)^{1/4}$.* We call the length ℓ_Q as the quantum length scale† $\ell_Q = (\kappa^3/\varepsilon)^{1/4}$ and define a corresponding wavenumber as $k_Q = 2\pi/\ell_Q$. Physically, ℓ_Q marks the transition between quasiclassical scales for which quantization of circulation plays no role (or the "granularity" of QT does not matter) and the quantum scales for which quantum restrictions are essential.

The Kolmogorov cascade cannot proceed beyond k_Q because its very existence is a purely quantum effect. The transfer of turbulent energy farther down the scales is possible by a different mechanism mediated by the Kelvin wave cascade on individual vortex lines in incompressible flow (12) [although a bottleneck, analogous to the classical case (13), might develop around ℓ_Q (14)]. The dissipation mechanism for $k > k^*$ is the phonon emission by Kelvin waves in He II (15) or the excitation of Caroli–Matricon states in vortex cores in ^{3}He-B (16). For this range, L'vov and Nazarenko (17) derived (neglecting these dissipation mechanisms) the superfluid energy spectrum for $k > k_Q$ to be of the form

$$E(k) = C_{LN}\Lambda\kappa\varepsilon^{1/3}\Psi^{-3/2}k^{-5/3}, \qquad [1]$$

where $\Psi = 4\pi K\Lambda^{-1}\kappa^{-2}$, $K = \int E(k)dk$, the dimensionless number Λ is about 15 for He II and 12 for ^{3}He-B, and $C_{LN} = 0.304$ (18). Beyond k^*, there must be a cross-over to $E(k) \propto 1/k$, which is the form of the spectral energy for straight vortex lines. Length scales smaller than $2\pi/k^*$ are not relevant to

*The quantum length scales in He II (for which $\kappa \cong 0.997 \times 10^{-7}$ m^2/s) and ^{3}He-B (for which $\kappa \cong 0.662 \times 10^{-7}$ m^2/s) are of the same order as the Kolmogorov dissipation scale η in the normal liquid He I just above T_λ; indeed, $\nu \approx \kappa/6$ according to ref. 11. As in unitary Fermi gas [M. Zwierlein, "Quantum transport in strongly interacting fermi gases" in *International Workshop on Quantum Turbulence: Cold Atoms, Heavy Ions, and Neutron Stars, March 18–April 19, Seattle* (2019), vol. 1, p. 1.], this fact links two apparently unrelated physical quantities—the kinematic viscosity, ν, in the normal state and the quantum of circulation, κ, in the superfluid state, bridging classical and quantum-mechanical descriptions of liquid ^{4}He.

†In the literature, the term quantum length scale is often used for the mean distance between vortex lines in the tangle, $\ell = 1/\sqrt{L}$. Although a useful measure of the intensity of QT and density of vortex lines, it does not carry any information on whether or not the normal fluid is turbulent. We will later show that ℓ_Q and ℓ differ by no more than a factor of 2 in He II. We reserve the phrase for ℓ_Q because it is analogous to the dissipation length η and allows useful comparisons to be made of complementary phenomena in classical turbulence and QT.

the dynamical motion of vortex tangles. An alternative approach to calculating the high wavenumber spectrum considers the flow as compressible. Tanogami (19) studied superfluid turbulence in 3D via the Gross–Pitaevskii equation and exploited the analytical method of Onsager's "ideal turbulence" theory. He proposed a quantum energy cascade with k^{-3} scaling beyond the quantum length scale, induced by quantum stresses, which, interestingly, may include the Kelvin wave cascade.

Now, let us examine the evolution of the steady-state superfluid energy spectrum in a box of size D, assuming a sustained energy input at scale M (e.g., by a grid of mesh size M, $\xi_3, \xi_4 \ll M \ll D$) (Fig. 1). Any remnant vorticity (21) (e.g., vortex loops pinned on the grid surface, which is nearly always rough on these scales) becomes unstable by the Glaberson–Donnelly instability (22), leading to a vortex tangle when the critical flow velocity is exceeded. A steady-state superfluid energy spectrum develops after a transient, truncated at k^* by one of the mechanisms described above.

The actual form of the steady-state energy spectrum depends on the interplay between the two important scales, M and ℓ_Q. For small enough ε, $\ell_Q > M$, and so the Richardson cascade cannot operate. Energy is transferred down the scales via a Kelvin wave cascade or quantum stress cascade, until k^* is reached. This is the Vinen (ultraquantum) turbulence, where the vortex tangle is approximately random (Fig. 1, *Top*). The temporal decay of this turbulence, characterized by just one fixed length scale (quantized vortices in the tangle are assumed to be approximately evenly spaced), was first discussed by Vinen (23). On page 504, he wrote, "We shall now suppose that, if two oppositely directed vortex lines approach each other sufficiently closely, they can break up into small vortex rings in the manner suggested by Feynman (6) and eventually degenerate into thermal excitations" and argued that the vortex line density decays according to the equation

$$\frac{dL}{dt} = -\frac{\vartheta_2 \kappa}{2\pi} L^2 , \qquad [2]$$

where ϑ_2 is a constant of order unity, leading to $L(t) \propto 1/t$ for late times. This form of the temporal decay of L, once the energy input stops, is the fingerprint of the Vinen turbulence.

Let us now increase ε so that ℓ_Q becomes nominally smaller than M (Fig. 1, *Middle*). Assuming an interaction between scales á la the equipartition theorem, the spectrum to the left of M must acquire the k^2 form, but the situation to the right of M changes by developing an inertial range between M and ℓ_Q, with the energy transfer from the small to the large wavenumbers occurring quasiclassically via the Richardson cascade. With increasing ε, the inertial range of scales increases and contains most of the kinetic energy of superfluid turbulence; see the red spectrum in Fig. 1, *Bottom*. This is the Kolmogorov (quasiclassical) turbulence, containing large vortex structures which can be thought of as composed of vortex-line bundles, achieved by partial polarization of the tangle. At scales sufficiently larger than ℓ_Q, the shape of the energy spectrum is thus Kolmogorov's. How far in k this picture holds depends on the interplay between classical and quantum physics, since the latter starts to intervene when approaching $k_Q = 2\pi/\ell_Q$; thereon, the turbulent motion is discretized and governed by quantum physics, described by the dynamics of individual quantized vortices. The quasiclassical limit is very similar to 3D Navier–Stokes for HIT, where viscous dissipation acting at small scales of order η is replaced by one of the mechanisms discussed above. At scales smaller than ℓ_Q the turbulence is always ultraquantum.

A key point is that for classical turbulence in the unbounded case, there are only two length scales to consider: M and η. In superfluid turbulence, there is an additional important scale, ℓ_Q, which intervenes as described above. Pure superfluid turbulence therefore cannot be considered, in contrast to statements in the literature, a simple "prototype" of turbulence; despite the similarities, it is different and more complex than the classical case. Naturally, however, the quasiclassical part of the picture is the same as that of classical 3D HIT and its temporal decay follows predictions of the spectral decay model (10, 24, 25). It is applicable also for decaying vortex line density, L, since the quasiclassical relation $\varepsilon = \nu_{\text{eff}} (\kappa L)^2$, following from the Navier–Stokes equations, holds (20). Here κL is the quasiclassical vorticity and ν_{eff} denotes the effective kinematic viscosity. We present the experimental evidence for this relationship in *Cross-Over from the Vinen to Kolmogorov Forms*.

We note that this close correspondence of the Kolmogorov-type QT with the classical case suggests the plausibility that the intermittency corrections may be the same for classical 3D HIT and for Kolmogorov pure superfluid turbulence at scales sufficiently larger than ℓ_Q. We will comment more on it later.

Manifestations of Vinen and Kolmogorov Forms of QT. At present, there are no direct spectral measurements of superfluid turbulence at zero temperature (i.e., close enough to zero that the

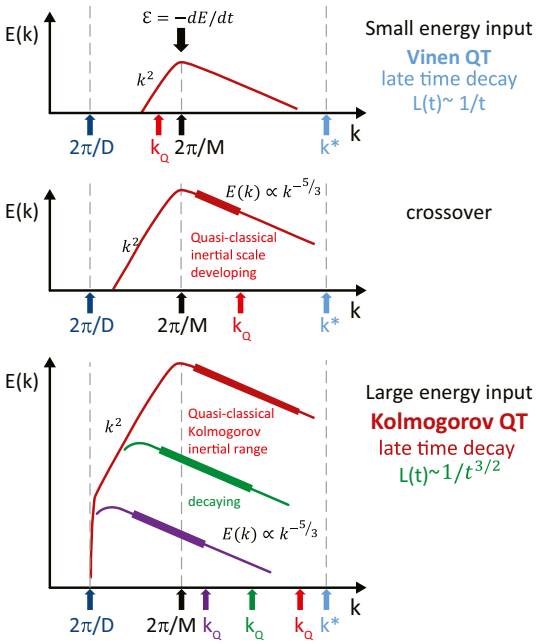

Fig. 1. Schematic in log-log coordinates of the general shapes of 3D energy spectra $E(k)$ plotted versus the wavenumber k of purely superfluid turbulence, assuming that it is forced at the scale M. (*Top*) Vinen turbulence, where ℓ_Q (red arrow) is larger than M. (*Middle*) Crossover from Vinen to Kolmogorov turbulence. With increasing ε, ℓ_Q crosses M. The classical Richardson cascade begins to operate and an inertial range of scales (thick red) develops gradually. (*Bottom*) For large enough ε, a significant extent of the inertial range develops as in steady-state classical 3D HIT (red). After the forcing stops, the decaying spectrum is shown in green and violet for two subsequent times; k_Q values are shown explicitly for each of them. The energy-containing scale grows during decay and eventually saturates at D and the classical decay of the form $L(t) \propto t^{-3/2}$ follows (20). Also, k_Q decreases faster than the energy-containing scale, so the inertial range shrinks with time. The spectra between k_Q and k^* have been drawn with slopes of $-5/3$ to be consistent with Eq. 1.

normal component is essentially nonexistent), so we cannot test the model in detail. Following Vinen (20), we introduce an effective mean-square vorticity in the superfluid component, defined by $\langle\omega^2\rangle_{\rm eff} = (\kappa L)^2$, which allows us to make direct reference to the experimentally measured quantity L. Using the above relation, we obtain the expression $L(t) \propto 1/t^{3/2}$ at late times for Kolmogorov QT when the length-scale saturation occurs; this is the result we shall test repeatedly here. The spectral form of the Vinen turbulence is not known [it could be of the $k^{-5/3}$ form as in Eq. **1** with a bottleneck or of the k^{-3} form of Tanogami (19)].[‡] For the purposes of Fig. 1, we take the manifestation of the Vinen turbulence to be Eq. **2**, according to which (at late times) $L \propto 1/t$. This is the main result we will test here. Our other important exploration concerns the cross-over between the two types of turbulence.

Cross-Over from the Vinen to Kolmogorov Forms. We will illustrate the cross-over in both steady-state and decaying quantum turbulence in ^{3}He-B in the measurements of the Lancaster group (27). QT was generated by oscillating grids and detected using the unique technique of Andreev reflection, which is possible because of the fermionic nature of superfluidity in ^{3}He-B. Briefly, the equilibrium number of quasiparticles (and quasiholes) can be sensed by a vibrating wire resonator. The drag force exerted on the vibrating wire by these ballistically propagating excitations is reduced if the wire is surrounded by a vortex tangle, as some incoming quasiparticles (quasiholes) cannot reach it, being Andreev reflected by energy barriers of the velocity field near the vortex cores.[§] The fractional decrease in damping can then be converted into the vortex line density in the tangle (27).

Two complementary experiments are worthy of attention. In the first one, quantum turbulence is generated by an oscillating grid of fine copper wires spaced $M = 50$ μm apart. By increasing the forcing, more and more energy is supplied to the flow at the scale M, all of which is being dissipated in the steady state. Facing the grid are detectors of quantum turbulence—two vibrating wire resonators—detecting the transition to quantum turbulence above a certain drive level (28). Increasing the oscillation amplitude of the grid results in a higher energy decay rate, ε; consequently, the quantum wavenumber $k_Q \propto \varepsilon^{1/4}$ increases. Bradley et al. (29) then investigated the temporal decay of vortex line density originating from various levels of intensity of the steady state; they presented representative results in their figure 2. With increasing ε used to reach the steady state, temporal decay changed its form from $L(t) \propto t^{-1}$ (Vinen QT) to $L(t) \propto t^{-3/2}$ (the Kolmogorov QT in a bounded domain).[¶]

In the second experiment, Bradley et al. (31) measured directly the energy decay rate ε of grid-generated turbulence inside a small box acting as a black body radiator of quasiparticles. The late-time decay changes in character, from $\varepsilon \propto t^{-2}$ to $\varepsilon = \nu_{\rm eff}\kappa^2 L^2 \propto t^{-3}$—consequently the turbulent energy decays as $K \propto t^{-2}$, in agreement with the late decay of turbulent energy in classical 3D HIT in a bounded domain. We emphasize that this experiment provides a direct measurement of the energy released by freely decaying quantum turbulence. It is remarkable that, leaving aside caveats such as homogeneity and isotropy of the turbulence inside the black box radiator, the decay of pure superfluid turbulence was found to be surprisingly similar to the known decay of classical 3D HIT. The results also confirm that the key phenomenological relationship, $\varepsilon = -dK/dt = \nu_{\rm eff}(\kappa L)^2$, first suggested by Vinen (20), is meaningful for the Kolmogorov type of pure superfluid turbulence.

We now consider another indication of the transition from Vinen to Kolmogorov turbulence in pure superfluid, following the scenario of Fig. 1, this time in He II. It is based on the observation of three critical velocities marking cross-overs between different types of flow due to the oscillating quartz tuning fork that resonates at 6.5 kHz, with prongs 3.50 mm long and a 90×75-μm cross-section (32). The first critical velocity of about 2 cm/s is hydrodynamic in origin, related to the formation of a vortical boundary layer, and therefore not directly relevant to turbulence in the bulk liquid.[#]

The second critical velocity can be linked reliably to significant production of quantized vorticity, which then propagates away from the surface of the tuning fork (or similar oscillators such as vibrating wires) and features a rapid increase in the drag force.[‖] The observed drag coefficients are typically 10^{-2} to 10^{-1}, much lower than in classical oscillatory flows, where drag coefficients of order unity are expected for cylinders or tuning forks at sufficiently high Reynolds number (or Keulegan–Carpenter number). This strongly suggests flow patterns significantly different from classical turbulence. No large flow structures resembling the classical wake exist in the superflow above the second critical velocity, which we therefore associate with the Vinen turbulence. It is only above the third critical velocity, about 1.5 m/s, that the drag coefficient starts to rise toward unity, the value typical for classical high Re flows. This is most likely related to a distinct change in the flow pattern, in which the superfluid develops larger polarized structures and starts to mimic the behavior of classical turbulent flows. We are therefore led to conclude that the third critical velocity marks the transition from Vinen- to Kolmogorov-type superfluid QT.

Pure Superfluid Turbulence in He II Driven at Small and Large Scales. Quantitative data on steady-state and decaying pure superfluid He II turbulence have been obtained by Golov and coworkers (34–36). They injected negative ions into the experimental

[‡]Although the energy spectrum beyond ℓ_Q has not yet been measured, a hint of possible k^{-3} scaling at high k appears in the Andreev reflection data (figure 13 in ref. 26) on the vorticity deduced for grid turbulence in ^{3}He-B.

[§]At very low temperatures below about 0.2 T_c the mean-free paths of these excitations—quasiparticles and quasiholes, the constituents of the normal fluid of ^{3}He-B—exceed the size of the turbulent box; hydrodynamic description of the normal fluid is therefore meaningless. The interaction of vortex line defects in the superfluid component of ^{3}He-B with the normal fluid thus must be described in terms of scattering of individual quasiparticles.

[¶]The cross-over corresponds to a steady-state level generated by grid velocity about 5 mm/s, when the grid is forced by about 0.2 μN (30). Multiplying these values gives the absolute energy decay rate in the stationary case. Knowing the size of the grid, we estimate that the decay takes place in a volume of order 5×10^{-8} m^3. With the density of ^{3}He-B ≈ 100 kg/m^3 this gives $\varepsilon \approx 2 \times 10^{-4}$ m^2/s^3, resulting in $\ell_Q = 2\pi(\varepsilon/\kappa^3)^{-1/4} \approx M$.

[#]Schmoranzer et al. (32) collected evidence from various complementary experiments employing small objects oscillating in He II in the zero-temperature limit and argued that the first critical velocity, connected mostly to frequency shifts rather than changes in the drag force, is associated with the formation of a number of quantized vortex loops near the surface of the oscillator, possibly forming a thin layer, which affects the coupling to the fluid and thus the hydrodynamic added mass.

[‖]Its magnitude is about 6 cm/s if measured at 6.5 kHz, using the fundamental vibrating mode of the fork, and about 12 cm/s if measured at 39.8 kHz, using the overtone, satisfying the scaling with the square root of oscillating frequency (33).

cell by a sharp field-emission tip and manipulated them by an electric field. This technique can be used for both the generation and detection of quantum turbulence. We focus first on the pure superfluid turbulence generated by impulsive spin-down, in which a rotating cubic-shaped container of He II, 4.5 cm in size, is brought rapidly to rest. For all starting angular velocities ($0.05 \leq \Omega \leq 1.5$ rad/s) (34), observed decays are of the form $L(t) \propto t^{-3/2}$, expected for late decay in classical 3D HIT decaying in the bounded domain—a strong signature of Kolmogorov-type QT.

Let us now consider temporal decay of pure superfluid turbulence with relatively low starting vortex line density, generated using an alternative technique of a jet of charged vortex rings of size about 1 μm, resulting from the injection of negative ions. At late times, two distinctly different power law decays were observed, depending on experimental conditions and the history of preparing the initial vortex tangle. Basically, instances of QT produced after short injection of ions display $L(t) \propto 1/t$ decay, while those generated after sufficiently long injection follow $L(t) \propto t^{-3/2}$ decay law at late times, in agreement again with Kolmogorov's pure superfluid turbulence generated by the rapid spin-down technique.

The phenomenological explanation within our model is as follows. For short charging times, the turbulent energy is supplied to the flow at the scale given by the typical size, 1 μm, of small vortex rings injected to the flow. The situation is basically the same as in Fig. 1, *Top*, with the size of the injected rings playing the role of the mesh size of the grid, *M*. The result is the Vinen turbulence with its typical signature, the $L(t) \propto 1/t$ form of the late decay. On the other hand, if the tangle of the same vortex line density is prepared by long charging times, the injected vortex rings have plenty of time to interact with each other (for more details, see ref. 14 and numerical simulations therein) as well as with the already existing vortex tangle. During the reconnection processes, both smaller and larger vortex loops are created, the former quickly propagating and decaying and the latter eventually creating large energy-containing superfluid eddies. This way, a superfluid energy spectrum is formed whose large scales have a form similar to classical turbulence. This results in the $L(t) \propto t^{-3/2}$ form of the late decay, a typical signature of the Kolmogorov turbulence in contained domains.

Situations intermediate to these two limiting cases are also possible, depending on the duration of charging, for which QT is neither of the Vinen nor of the Kolmogorov type. When charging is stopped, the vortex line density first roughly obeys the Vinen $L(t) \propto 1/t$ type of decay (corresponding to the decay of energy contained in small eddies of the size of order ℓ_O), displays a cross-over, and enters the $L(t) \propto t^{-3/2}$ regime.

Quantum Turbulence in the Two-Fluid Regime

At finite temperatures, He II and ^{3}He-B behave as two-fluid systems consisting of the inviscid superfluid and viscous normal components having their separate velocity fields. We emphasize that the presence of the normal fluid renders the issue more complex.

The first step in the phenomenological description is to determine which fluid is turbulent. With no vortex lines, the superfluid component under isothermal conditions flows independently of the normal fluid possessing a kinematic viscosity $\nu_n = \mu/\rho_n$, where μ is the dynamical viscosity of the entire liquid. Potential superflow can be superimposed on the normal fluid flow. Although this ideal situation is uncommon, there is experimental evidence in flow of He II around oscillatory objects for classical instabilities in the normal fluid flow before the critical velocity for Glaberson–Donnelly instability is reached in the corresponding superflow (37). If vortex lines are present, they couple the two velocity fields by the action of the mutual friction force, acting at all length scales. This has the serious consequence of creating superfluid energy spectra of shapes drastically different from those at $T \to 0$.

Superfluid Turbulence in Stationary Normal Fluid of ^{3}He-B. This case represents the next logical step in the phenomenological description of QT because of its simplicity. The simplicity arises from the relatively high kinematic viscosity of the normal fluid of ^{3}He-B, which renders the normal fluid effectively stationary. ** Although we formally deal with two velocity fields, the velocity field of the normal fluid only determines the unique and physically significant frame of reference in which the normal fluid is at rest.

Experiments with ^{3}He-B have to be performed at sub-milliKelvin temperatures; to keep the flow so cold, the energy input needs to be very modest, typically of the order a few nanowatts. It is this factor and the high viscosity of the normal fluid that ensure that the normal fluid remains at rest with respect to the experimental container. The vortex lines will thus not move freely but are subject to a friction force as they move; this friction is temperature dependent and becomes larger as $T \to T_c$ (38). We should therefore expect that superfluid turbulence considered in the earlier section in the zero-temperature limit will be modified by the presence of damping: Vortex lines will appear smoother and short Kelvin waves and vortex cusps resulting from reconnections will be quickly damped out. With increasing temperature the damping becomes so strong that above $\approx 0.6 T_c$ quantum turbulence does not exist. Temperature thus plays a similar role here as the inverse Reynolds number in classical turbulence (39).

The energy spectrum of the turbulent superfluid possesses the following special features: 1) There is a maximum size of the turbulent eddy limited by mutual friction (40), and 2) dissipation due to mutual friction occurs at all length scales and 3) modifies the roll-off exponent to −3 at largest scales which, according to predictions of continuum approximation, displays a cross-over to the classical −5/3 (40, 41). Let us emphasize, however, that these results have been obtained theoretically within the continuum approximation, i.e., assuming that all relevant length scales of the problem are sufficiently larger than ℓ and the energy input occurs at large scales. These features are yet to be investigated in detail experimentally.

Quantum Turbulence in He II above ≈1 K. Here He II displays the two-fluid behavior. Isothermal incompressible flow of the normal fluid of He II can be described using the Navier–Stokes equations with density ρ_n and very low kinematic viscosity of order κ, characterized by the analogue of the Reynolds number in classical viscous fluids: the Donnelly number, Dn, which is based on the kinematic viscosity of the normal fluid alone, $\nu_n = \mu/\rho_n$, not on the kinematic viscosity $\nu = \mu/\rho$ of the entire fluid.††

**We assume here that the hydrodynamic description of the normal fluid of ^{3}He-B is justified; i.e., the mean-free path of its constituents, viz. quasiparticles and quasiholes, is short; in practice, this means that the temperature is above about 0.3 T_c.

††This dimensionless parameter, a "Reynolds number" defined for the normal component of He II only, was named by Schmoranzer et al. (37) as the Donnelly number, based on the latter's early investigations of boundary layer flows of He II.

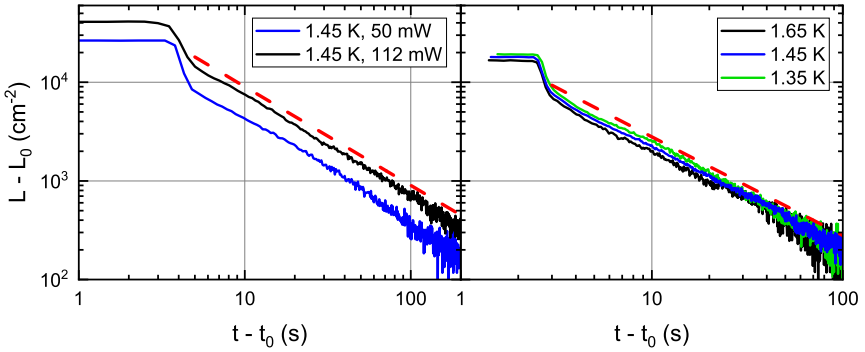

Fig. 2. Temporal decay of vortex line density (*Left*) in spherical counterflow generated by a steady-state central heater and (*Right*) generated mechanically by a vibrating fork. In both panels, t_0 is a virtual origin of time and L_0 denotes the remnant vorticity. Red dashed lines have the slope $1/t$ to guide the eye.

Schmoranzer et al. (37) used this nomenclature for oscillatory flows at high Stokes numbers, but we extend its definition for any quantum flow of superfluid helium and suggest that its meaning is the same for the normal fluid flow as that of the Reynolds number in classical flows. Flow of the superfluid component of He II is potential. In isothermal flow of He II, the normal and superfluid velocity fields are independent but become coupled by the mutual friction force when quantized vortices appear in the superfluid. Additionally, any temperature gradient in He II results in a thermal counterflow of the normal and superfluid components against each other which we shall consider in detail later.

From the fluid-dynamical point of view, the situation in He II differs from that in ^{3}He-B because the normal fluid is much less viscous. Additionally, the mutual friction force (characterized by the dissipative mutual friction parameter α) (42) at temperatures far enough away from T_λ is typically weaker by one to two orders of magnitude than in ^{3}He-B above $\approx 0.3T_c$, considered above. It therefore seems sensible to check whether the physical picture of two nearly independent velocity fields agrees with some experimental observations. We first focus on the isothermal and mechanically driven flows of He II.

It is often stated in the literature that the mechanically driven He II, with both components forced in the same way, results in the so-called coflow and represents Kolmogorov-type QT. This, however, is generally not the case. Experimental evidence on this point comes from a recent Prague experiment. QT is driven mechanically by a small quartz tuning fork with prongs of small $(75 \times 90)\ \mu m^2$ cross-section. Fig. 2, *Right* shows that $L(t) \propto 1/t$, the late temporal decay of the Vinen type, in accordance with Fig. 1, *Top*, where the flow is driven at a scale smaller than or comparable to ℓ_Q.[‡‡] The normal fluid is therefore driven by the fork at scale smaller than η_n, for which the classical phenomenology is hardly applicable. The situation is somewhat as in ^{3}He-B, but without the unique quiescent normal fluid frame; the normal fluid flow is characterized by Dn = 17, which is slightly past the classical instability (37). Mutual friction is weak and does not significantly affect the decay.

It is fair to note that QT generated by an oscillating fork is far from HIT, so the experimental results should be interpreted with care. The nonhomogeneous tangle is expected to undergo a decay process accompanied by vortex diffusion. However, convincing experimental evidence was provided by Milliken et al. (43), who used the technique based on pulses of negative ions propagating through the steady state and decaying vortex tangles generated by ultrasound. The pulses were shaped by gate grids and manipulated by electric field, so that they could be stopped at a chosen position to provide spatial as well as temporal information on the decay. An overall inverse time decay of L was observed, which seemed to preserve its spatial profile, indicating that local decay dominates over diffusive phenomena. Under such an assumption, the nonlinear decay rate $\propto L^2$ would first lead to a rapid homogenization of the tangle, which would further decay as $L(t) \propto t^{-1}$.[§§]

Kolmogorov Quantum Turbulence in Coflowing He II. Consider now QT in coflowing He II at $T > 1$ K. Perhaps surprisingly, it has properties closely similar to those of 3D HIT in classical fluids. In contrast with ^{3}He-B, the normal fluid of He II becomes readily turbulent: There are not one but two turbulent velocity fields, coupled by the mutual friction force, acting at all relevant length scales. We are dealing here with the situation of double turbulence and have to examine both the superfluid and the normal fluid energy spectra.

Let us consider the example of turbulent He II flow driven by a grid at mesh scale $M \gg \ell_Q$. To simplify the problem, let us artificially switch off the mutual friction and assume that the temperature is just below 1.5 K, where $\nu_n \approx \kappa$ (42)—in other words, the Donnelly number is equal to the superfluid Reynolds number. It follows that ℓ_Q in the superfluid is equal to the Kolmogorov dissipation scale η_n in the normal fluid and that the turbulent spectra in the normal fluid and in the superfluid are naturally matched at scales considerably larger than ℓ_Q or η_n. The difference is that while in the normal fluid the Richardson cascade is terminated at this scale, it continues in the superfluid in the form of a Kelvin wave or quantum stress cascade, and the dissipation occurs beyond $k^\star$ introduced above. Upon decreasing (increasing) the temperature, due to the steep temperature dependence of $\nu_n(T)$, η_n becomes larger (smaller) than ℓ_Q. By turning on the mutual friction, not much happens at large scales (significantly exceeding η_n or ℓ_Q, whichever is larger), as large eddies of normal and superfluid components are

[‡‡]At $T = 1.35$ and 1.45 K the Kolmogorov dissipation scale in the normal component, η_n, is even larger and, at 1.65 K, about equal to ℓ_Q.

[§§]While this scenario is contrary to the claim that the spatial profile is maintained during decay, it is surprisingly consistent with the raw data in figure 2 of ref. 43, where in the center of the cell, the initially high L drops by a factor of ≈ 4.5 within the first 4 s, while in the border regions a significantly smaller drop by a factor of ≈ 2 is observed. This validates the scenario of predominantly local decay of nonhomogeneous QT, which results in $L(t) \propto t^{-1}$ at late times.

closely matched. Upon approaching smaller and smaller scales, however, the matching cannot be complete, dissipation due to mutual friction starts to operate (the roll-off exponent becomes gradually steeper), and one component starts to act as a source or drain for the other. This results in an increase of intermittency corrections, as predicted by Boue et al. (44) and experimentally confirmed by Varga et al. (45).

Both the superfluid and normal energy spectra in steady-state and decaying Kolmogorov turbulence of He II contain an inertial range of scales. This has been observed in a number of coflow experiments, first by Maurer and Tabeling (46) in the von Kármán flow and by Roche and coworkers (47) in superfluid wind tunnels (48). In these experiments, velocity fluctuations were determined using a Pitot tube, and the characteristic $f^{-5/3}$ frequency dependence of the spectrum was observed; this scaling corresponds to $E(k) \sim k^{-5/3}$, if one uses Taylor's frozen flow hypothesis, and confirms the presence of a Richardson energy cascade as in classical turbulence. Geometrically it means that the turbulence contains, within a tangle of random vortex lines, partially polarized vortex lines, or bundles, with relatively large coarse-grained superfluid vorticity. We also note that the inertial range in the turbulent normal fluid was observed by Guo and coworkers (45) by visualizing grid-generated turbulence using neutral He2* molecules, allowing one to measure transverse velocity structure functions selectively in the normal fluid. This is possible due to the small size of He2* triplet molecules that are effectively part of the normal fluid and do not trap vortex lines above $\approx$1 K (49).

Grid-generated QT in He II, driven at the large-scale M, when both components are turbulent on scales appreciably larger than ℓ_Q, represents a typical example of Kolmogorov QT. Large normal and superfluid scales are closely coupled by mutual friction, which does not cause any appreciable energy loss and, in accordance with Richardson's picture, there is an inertial range characterized by the $-5/3$ exponent (neglecting intermittency). Matching is not possible once the quantum or Kolmogorov length scale is reached. Mutual friction partly dissipates and partly transfers the turbulent energy from superfluid eddies to normal ones and vice versa, with either fluid serving as the drain or source of energy for the other. Viscous dissipation, together with the coupling by dissipative mutual friction, terminates both normal and superfluid cascades. The Kelvin wave or quantum stress cascades, so important in the zero-temperature limit, do not play a significant role here. Turbulent coflowing He II above about 1 K can thus be treated, at least approximately, as a single-component quasiclassical fluid, characterized by the temperature-dependent effective kinematic viscosity $\nu_{\rm eff}$. Its value can be extracted from the temporal decay, when $L(t)$ displays the universal form of the decay [as observed in many experiments (10, 24, 25, 50–52) and reviewed in ref. 25]:

$$L(t+t_0) = L(\tau) = \frac{3\sqrt{3}D}{2\pi\kappa}\sqrt{\frac{C^3}{\nu_{\rm eff}}}\tau^{-3/2}. \qquad [3]$$

Here t_0 is the virtual origin time marking the instant when L would be infinite if this law of decay were to be valid, and D is the size of the turbulent box (playing the role of saturated energy-containing length scale). This decay is the typical quasiclassical signature (20) of the Kolmogorov QT, allowing us to extract $\nu_{\rm eff}(T)$; see also the more rigorous recent treatment based on independent measurements of decaying turbulence in the superfluid and normal components of He II (52, 53).

Thermal Counterflow of He II. The flow of He II can take various forms because of the existence of two fluid components. One can push the normal fluid and the superfluid components to flow with different average velocities, a situation generally called counterflow. A special case of counterflow is the thermal counterflow, easily achieved in a channel closed at one end and open to the He II bath at the other. Heat flux q supplied at the closed end is carried away by the normal fluid, with the superfluid flowing in the opposite direction so that the net mass flux is zero. The counterflow velocity $u_{\rm ns} = q/(\rho_s \sigma T)$ is established, where σ is the entropy of He II. QT appears in the channel when q exceeds a critical value.

It has been known since early experiments, notably those performed by Tough's group (56), that counterflow turbulence can exist in two forms, referred to as T I and T II. Recently Guo and coworkers (49, 57), using helium excimer molecules as tracers of the normal fluid, revealed that the normal fluid in the T II state is turbulent. In the T I state, where the flow of the normal component is laminar beyond reasonable doubt, the turbulent energy is injected around ℓ_Q by the reconnection-based mechanism first identified by Schwarz (54, 55). The superfluid energy spectrum therefore has the shape as sketched in Fig. 3, *Top*. The shape is the same as in Fig. 1, *Top*. For small enough ε we deal with Vinen turbulence, the decay of which was experimentally confirmed (58) to obey $L(t) \propto t^{-1}$ at late times.

The two forms of QT in He II—Vinen and Kolmogorov—display two distinctly different forms of decay which subsequently allow the definition of two effective kinematic viscosities of turbulent He II. In addition to $\nu_{\rm eff}(T)$ introduced above for Kolmogorov QT, we now follow refs. 36 and 52 and note that the energy per unit mass associated with a random tangle of vortex lines in Vinen QT (i.e., superflow circulating with velocity $\kappa/(2\pi r)$ around vortex lines) is given by $(\rho_s\kappa^2)/(4\pi\rho)\, L \ln(\ell/\xi_4)$, where $\ell = 1/\sqrt{L}$ denotes the mean intervortex distance in the tangle. By differentiating with respect of time and using Eq. **2**, we see that the turbulent energy would then decay as $\varepsilon = \nu' \kappa^2 L^2$, where the quantity

$$\nu' = \frac{\vartheta_2 \rho_s}{8\pi^2\rho}\kappa \ln(\ell/\xi_4) \qquad [4]$$

is the effective kinematic viscosity for the Vinen-type QT.

We thus have two definitions for two effective kinematic viscosities ν' and $\nu_{\rm eff}$, which can be extracted from decaying turbulent He II flow of the Vinen and Kolmogorov forms. Their existence is not a consequence of the two-fluid behavior, since they readily exist in the $T \to 0$ limit as well. And they need not be the same, either. Indeed, while $\nu_{\rm eff}$ is a property of turbulent flow of the entire He II, i.e., of both fluids whose turbulent motions are coupled at large enough scales, ν' is the property of a single fluid flow, namely of the turbulent superfluid component, coupled by the mutual friction force to the normal fluid. This difference—coupling to the normal fluid as well as the factor ρ_s/ρ—should disappear with dropping temperature, as ρ_s approaches ρ and the mutual friction gradually ceases to operate. For reasons such as ill-defined boundary conditions in He II below 1 K, the values of ν' and $\nu_{\rm eff}$ are so far not determined with sufficient accuracy to unequivocally confirm that ν' equals $\nu_{\rm eff}$ at low temperature; however, they both have been found to be of order 0.1κ (51).[¶¶]

[¶¶]Discussion of boundary conditions for turbulent flows of helium superfluids is outside the scope of this paper. In short, there is experimental evidence that both in He II (51) and in ^{3}He B (59) the turbulent flow with dropping temperature decouples from the container reference frame.

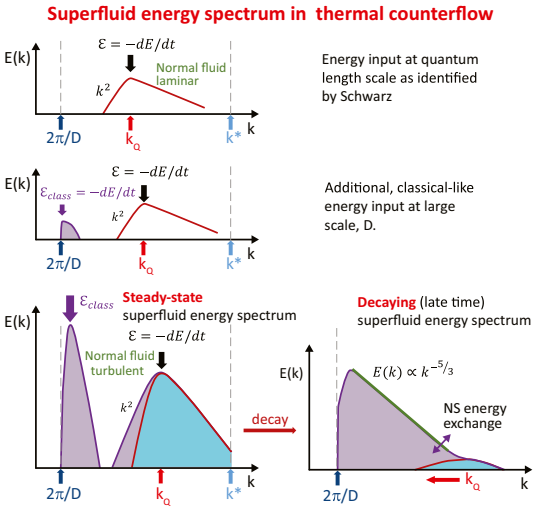

Fig. 3. Schematic view in log-log coordinates of the general shapes of 3D superfluid energy spectra of thermal counterflow turbulence in He II. (*Top*) Vinen turbulence, where the energy input identified by Schwarz (54, 55) occurs at $\ell_Q = 2\pi/k_Q$ (red arrow). The temporal decay is of the form $L(t) \propto 1/t$. (*Middle*) Upon increasing the heat flux, there is additional quasiclassical energy input in the normal component at large scale which, because of mutual friction, occurs in the superfluid component as well. (*Bottom Left*) With increasing heat input, there is energy input at large scale akin to classical turbulence, but the inertial range of the Kolmogorov-type QT, characterized by the −5/3 roll-off exponent, cannot develop, as mutual friction acts on all scales making the roll-off in this range much steeper. There is still a quantum peak because of the energy input at quantum length-scale ℓ_Q, which itself shifts to the right with increasing heat input. (*Bottom Right*) Once the heat flux ceases, the quantum energy peak quickly decays and the energy content at large scales gradually cascades down the scales, forming an inertial range that acquires classical Kolmogorov form. It results in a classical decay of the form $L(t) \propto 1/t^{3/2}$, with growing quantum length-scale ℓ_Q.

At this point, we need to discuss the relation between the quantum length scale, defined as before quasiclassically as $\ell_Q = (\kappa^3/\varepsilon)^{1/4}$, and the mean intervortex distance $\ell = 1/\sqrt{L}$, as this quantity is also often referred to in the literature as quantum length scale. It is easy to show that for Kolmogorov turbulence in He II they are roughly equal. Indeed, assuming the validity of the above quasiclassical relationship $\varepsilon = \nu_{\text{eff}}(\kappa L)^2$ (20), we obtain their ratio to be

$$\frac{\ell_Q}{\ell} = \left(\frac{\kappa}{\nu_{\text{eff}}}\right)^{1/4}. \qquad [5]$$

Available experimental data on $\nu_{\text{eff}}(T)$ (51, 53, 60, 61) suggest that in He II over most of the temperature range ℓ_Q and ℓ differ by less than a factor of 2.

Let us now return to counterflow turbulence. Upon increasing the heat load, there develops an instability of laminar flow that carries the heat away from the heater, and the transition to turbulence occurs in the normal fluid (as in any channel or pipe flow of classical viscous fluid) to which the energy is injected quasiclassically, at the outer scale of order the size of the counterflow channel, D. An inertial range of scales with the classical roll-off exponent of −5/3 cannot be established in the normal fluid. The reason is that mutual friction creates superfluid eddies and couples them with normal eddies and also dissipates the turbulent energy at all scales. This mutual friction mechanism serves as an additional source of energy injection to the superfluid component, at large scales, resulting in the gradual growth of a classical-like peak, as sketched in Fig. 3, *Middle*; the situation for increasing heat input is shown in Fig. 3, *Bottom*. The sketch takes into account that eddies larger than D cannot exist and that steady-state measurements of the structure functions (49, 57) suggest a steeper roll-off exponent of its right-hand side. Of course, the steady energy input into the superfluid component identified by Schwarz (54, 55) operates and results in a quantum peak in the superfluid energy spectrum around ℓ_Q. Its low wavenumber end is again of the k^2 form because of the equipartition theorem (62).

This steady-state, two-peak shape of the superfluid energy spectrum drastically changes during the temporal decay that occurs when heating is switched off. For a short transition time, counterflow is still driven by the excess entropy contained in the channel; for details, see refs. 63 and 64. The quantum peak quickly decays, displaying a decay of the $L \propto 1/t$ type. Simultaneously, over times of the order of the turnover time of large eddies, the energy contained at large scales of both fluids proceeds through the inertial range of scales. From now on, the inertial range is characterized by the classical −5/3 roll-off exponent, as superfluid and normal eddies are coupled at these scales; thus, hardly any significant dissipation occurs, with the situation being similar to that in the coflow (Kolmogorov) QT. As the energy reaches smaller and smaller scales, a larger number of vortex lines are needed for carrying nearly the same energy content. This is displayed as a "bump" in recorded decay curves of $L(t)$. The quasiclassical decay occurs beyond this point, displaying $L(t) \propto t^{-3/2}$ (58, 62).

The dynamics of vortex tangles in thermal counterflow are not fully understood by any means. Their complexity can be illustrated by an experimental study of thermal counterflow in a channel when the turbulence was not allowed to settle to a statistical steady state (64). This was achieved by modulating by a square-wave $\dot{q}$ and a similarly varying counterflow velocity u_{ns}. The turbulent transients thus obtained allowed one to study, by using the phase portrait, the time evolution of both the growth and decay of L. In particular, while the growth of L always followed the same form, independent of the length of the heat pulse, the temporal decay of vortex line density was strongly affected by the history of the turbulent sample (figure 7 in ref. 64). The bump in decaying $L(t)$ was displayed only in decays of dense original tangles, prepared using long heat pulses sufficient for generating large eddies and, with the aid of mutual friction, the classical-like part of the superfluid energy spectrum. The situation is similar to that discussed earlier, when the tangle was generated in the $T \to 0$ limit by the injection pulses of ions (immediately creating small vortex rings) of variable duration (36). In both these cases the decay of $L(t)$ depends on the shape of the superfluid energy spectrum (also on the shape of the energy spectrum in the normal fluid in the case of thermal counterflow, due to coupling by the mutual friction force); these shapes depend on how intensely and on which length scales QT is driven.

Let us add that this phenomenological scenario of thermal counterflow and its decay, complex though it is, derives indirect support from complementary experiments. First, the Prague group investigated in detail the steady-state (65) and temporal decay (66) of pure superflow in square channels, with ends covered by sintered silver superleaks, allowing a net throughflow of the superfluid component only (the normal fluid throughflow was suppressed by submicrometer pores of the sintered silver plugs). While the measurements of L in the steady states of counterflow and

pure superflow display the same value for the same mean counterflow velocity, the temporal decays are distinctly different. The experimentally recorded bump on $L(t)$ decay curves originating from pure superflow is suppressed, either fully or at least significantly. The reason is easily understood: In pure superflow the classical energy input at large scale of order D is inefficient, as there is no net flow of the normal component through the channel.

In the second example, the Prague group utilized an experimental cell of the outside form of a regular dodecahedron containing a spherical sample of He II. The heat, supplied by a small spherical heater in the center, generates a nearly spherical counterflow. Upon exceeding some critical heating level, an inhomogeneous vortex tangle is formed and surrounds the spherical heater. A full account of this experiment will be published elsewhere, but preliminary second sound data display temporal decay of the form $L(t) \propto 1/t$, where $L(t)$ now stands for the spatially averaged vortex line density, detected by a chosen spherical resonant harmonic of second sound, as shown in Fig. 2, *Left*. Assuming local decay, this is a typical signature of Vinen type of quantum turbulence. It is important to emphasize that this decay form follows the steady-state vortex line density values which, in conventional 1D thermal counterflow, would have displayed a complex decay containing a bump and subsequent quasiclassical late decay $\propto t^{-3/2}$. The reason for this distinctive difference is the lack of classical large-scale energy input that in the "conventional" 1D counterflow occurs due to the friction between the normal fluid and solid channel wall. Such an energy input does not exist in spherical counterflow with radial normal fluid flow.

Conclusions

We have presented a unified phenomenological description of various forms of QT in helium superfluids. We believe that all forms of QT observed to date, and their relation to classical turbulence in viscous fluids, are broadly understood at this phenomenological level. In particular, we presented a unified description on the existence of the Vinen and Kolmogorov forms of QT. Their existence is not a consequence of the two-fluid behavior of quantum fluids; they readily exist as two different forms of pure superfluid turbulence in the zero-temperature limit. These two forms emerge as a direct consequence of quantum mechanical constraint on circulation in a superfluid, which results in the existence of a finite quantum length scale. We have discussed a crossover from one form of QT to the other. The very existence of the quantum length scale makes even pure superfluid turbulence more complex than classical turbulence in viscous fluids.

At finite temperature, the presence of the normal fluid, whether turbulent or not, adds more complexity to existing forms of quantum turbulence and their temporal decays. Although the phenomenology presented here is semiquantitative at best, this unified picture captures many experimental facts, known features, and regimes of quantum turbulence accumulated over many years of research of helium superfluids, both in the limit of zero temperature and in the temperature range where they display two-fluid behavior. We therefore believe that our perspective represents a firm basis for fluid-dynamical studies of even more complex turbulent superfluid systems, such as mixtures of Bose–Einstein condensates, heavy atomic nuclei, and neutron stars.

Data Availability. All study data are included in this article.

Acknowledgments

We thank our many colleagues, too numerous to name here, for fruitful collaboration and stimulating discussions over the years. This research is funded by the Czech Science Foundation under Project GAČR 20-00918S. D.S. and S.M. acknowledge support for the experimental work with tuning-fork microresonators under Project GAČR 20-13001Y.

1 U. Frisch, *Turbulence: The Legacy of A. N. Kolmogorov* (Cambridge University Press, 1995).
2 L. Skrbek, K. R. Sreenivasan, Developed quantum turbulence and its decay. *Phys. Fluids* **24**, 011301 (2012).
3 C. F. Barenghi, L. Skrbek, K. R. Sreenivasan, Introduction to quantum turbulence. *Proc. Natl. Acad. Sci. U.S.A.* **111**, 4647 (2014).
4 D. R.Tilley, J. Tilley, *Superfluidity and Superconductivity* (Institute of Physics Publishing, 1986).
5 L. Onsager, In discussion on paper by C. J. Gorter. *Nuovo Cimento* **6** (suppl. 2), 249 (1949).
6 R. P. Feynman, "Application of quantum mechanics to liquid helium" in *Progress in Low Temperature Physics*, C. J. Gorter, Ed. (North Holland, Amsterdam, The Netherlands, 1955), vol. 1, pp. 493–515.
7 G. Birkhoff, Fourier synthesis of homogeneous turbulence. *Commun. Pure Appl. Math.* **7**, 19 (1954).
8 P. G. Saffman, The large-scale structure of homogeneous turbulence. *J. Fluid Mech.* **27**, 581 (1967).
9 K. R. Sreenivasan, On the universality of the Kolmogorov constant. *Phys. Fluids* **7**, 27788 (1995).
10 S. R. Stalp, L. Skrbek, R. J. Donnelly, Decay of grid turbulence in a finite channel. *Phys. Rev. Lett.* **82**, 4831 (1999).
11 V. S. L'vov, L. Skrbek, K. R. Sreenivasan, Viscosity of liquid 4He and quantum of circulation: Are they related?. *Phys. Fluids* **26**, 041703 (2014).
12 B. Svistunov, Superfluid turbulence in the low-temperature limit. *Phys. Rev. B* **52**, 3647 (1995).
13 D. A. Donzis, K. R. Sreenivasan, The bottleneck effect and the Kolmogorov constant in isotropic turbulence. *J. Fluid Mech.* **657**, 171–188 (2010).
14 P. C. diLeoni, P. Mininni, M. E. Brachet, Dual cascade and dissipation mechanisms in helical quantum turbulence. *Phys. Rev. A* **95**, 053636 (2017).
15 W. F. Vinen, Decay of superfluid turbulence at a very low temperature: The radiation of sound from a Kelvin wave on a quantized vortex. *Phys. Rev. B* **64**, 134520 (2001).
16 M. A. Silaev, Universal mechanism of dissipation in Fermi superfluids at ultralow temperatures. *Phys. Rev. Lett.* **108**, 045303 (2012).
17 V. S. L'vov, S. Nazarenko, Spectrum of Kelvin-wave turbulence in superfluids. *JETP Lett.* **91**, 464 (2010).
18 L. Boue *et al.*, Exact solution for the energy spectrum of Kelvin wave turbulence in superfluids. *Phys. Rev. B* **84**, 064516 (2011).
19 T. Tanogami, Theoretical analysis of quantum turbulence using the Onsager "ideal turbulence" theory. arXiv:2009.11057v1 (23 September 2020).
20 W. F. Vinen, Classical character of turbulence in a quantum liquid. *Phys. Rev. B* **61**, 1410 (2000).
21 D. D. Awschalom, K. W. Schwarz, Observation of a remanent vortex-line density in superfluid helium. *Phys. Rev. Lett.* **52**, 49–52 (1984).
22 W. I. Glaberson, W. W. Johnson, R. M. Ostermeier, Instability of a vortex array in He II. *Phys. Rev. Lett.* **33**, 1197 (1974).
23 W. Vinen, Mutual friction in a heat current in liquid helium II. III. Theory of the mutual friction. *Proc. R. Soc. Lond. A* **242**, 493–515 (1957).
24 L. Skrbek, S. Stalp, On the decay of homogeneous isotropic turbulence. *Phys. Fluids* **12**, 1997 (2000).
25 L. Skrbek, K. R. Sreenivasan, "How similar is quantum turbulence to classical turbulence"? in *Ten Chapters of Turbulence*, P. A. Davidson, Y. Kaneda, H. K. Moffatt, K. R. Sreenivasan, Eds. (Cambridge University Press, 2013), chap. 10.
26 V. Tsepelin *et al.*, Visualization of quantum turbulence in superfluid 3He-B: Combined numerical and experimental study of Andreev reflection. *Phys. Rev. B* **96**, 054510 (2017).
27 S. N. Fisher, G. R. Pickett, "Quantum turbulence in superfluid 3He at very low temperatures" in *Progress in Low Temperature Physics XVI*, M. Tsubota, W. P. Halperin, Eds. (Elsevier, 2009), vol. XVI, pp. 147–194.

28 D. I. Bradley *et al.*, Emission of discrete vortex rings by a vibrating grid in superfluid 3He-B: A precursor to quantum turbulence. *Phys. Rev. Lett.* **95**, 035302 (2005).
29 D. I. Bradley *et al.*, Decay of pure quantum turbulence in superfluid ^{3}He-B. *Phys. Rev. Lett.* **96**, 035301 (2006).
30 D. I. Bradley *et al.*, Vortex generation in superfluid He-3 by a vibrating grid. *J. Low Temp. Phys.* **134**, 381 (2004).
31 D. I. Bradley *et al.*, Direct measurement of the energy dissipated by quantum turbulence. *Nat. Phys.* **7**, 473 (2011).
32 D. Schmoranzer *et al.*, Multiple critical velocities in oscillatory flow of superfluid 4He due to quartz tuning forks. *Phys. Rev. B* **94**, 214503 (2016).
33 R. Hanninen, W. Schoepe, Universal onset of quantum turbulence in oscillating flows and crossover to steady flows. *J. Low Temp. Phys.* **158**, 410 (2010).
34 P. M. Walmsley, A. I. Golov, H. E. Hall, A. A. Levchenko, W. F. Vinen, Dissipation of quantum turbulence in the zero temperature limit. *Phys. Rev. Lett.* **99**, 265302 (2007).
35 P. M. Walmsley, A. I. Golov, Quantum and quasiclassical types of superfluid turbulence. *Phys. Rev. Lett.* **100**, 245301 (2008).
36 P. M. Walmsley, A. I. Golov, Coexistence of quantum and classical flows in quantum turbulence in the T=0 limit. *Phys. Rev. Lett.* **118**, 134501 (2017).
37 D. Schmoranzer *et al.*, Dynamical similarity and instabilities in high Stokes number oscillatory flows of superfluid helium. *Phys. Rev. B* **99**, 054511 (2019).
38 T. D. C. Bevan *et al.*, Vortex mutual friction in superfluid He-3. *J. Low Temp. Phys.* **109**, 423 (1997).
39 A. P. Finne *et al.*, Observation of an intrinsic velocity-independent criterion for superfluid turbulence. *Nature* **424**, 1022 (2003).
40 W. F. Vinen, Theory of quantum grid turbulence in superfluid ^{3}He-B. *Phys. Rev. B* **71**, 024513 (2005).
41 V. S. L'vov, S. V. Nazarenko, G. E. Volovik, Energy spectra of developed superfluid turbulence. *JETP Lett.* **80**, 479 (2004).
42 R. J. Donnelly, C. F. Barenghi, The observed properties of liquid helium at saturated vapor pressure. *J. Phys. Chem. Ref. Data* **27**, 1217 (1998).
43 F. Milliken, K. Schwarz, C. Smith, Free decay of superfluid turbulence. *Phys. Rev. Lett.* **48**, 1204 (1982).
44 L. Boue *et al.*, Enhancement of intermittency in superfluid turbulence. *Phys. Rev. Lett.* **110**, 064516 (2013).
45 E. Varga, W. Guo, J. Gao, L. Skrbek, Intermittency enhancement in quantum turbulence in superfluid 4He. *Phys. Rev. Fluids* **3**, 094601 (2018).
46 J. Maurer, P. Tabeling, Local investigation of superfluid turbulence. *Europhys. Lett.* **43**, 29 (1998).
47 J. Salort *et al.*, Turbulent velocity spectra in superfluid flows. *Phys. Fluids* **22**, 125102 (2010).
48 J. Salort, B. Chabaud, E. Leveque, P. E. Roche, Energy cascade and the four-fifths law in superfluid turbulence. *Europhys. Lett.* **97**, 34006 (2012).
49 A. Marakov *et al.*, Visualization of the normal-fluid turbulence in counterflowing superfluid He-4. *Phys. Rev. B* **91**, 094503 (2015).
50 S. Babuin, E. Varga, L. Skrbek, The decay of forced turbulent coflow of He II past a grid. *J. Low Temp. Phys.* **175**, 324–330 (2014).
51 D. E. Zmeev *et al.*, Dissipation of quasiclassical turbulence in superfluid 4He. *Phys. Rev. Lett.* **115**, 155303 (2015).
52 J. Gao, W. Guo, W. F. Vinen, Dissipation in quantum turbulence in superfluid He-4 above 1 K. *Phys. Rev. B* **97**, 184518 (2018).
53 J. Gao, W. Guo, W. Vinen, Determination of the effective kinematic viscosity for the decay of quasiclassical turbulence in superfluid He-4. *Phys. Rev. B* **94**, 094502 (2016).
54 K. W. Schwarz, Theory of turbulence in superfluid 4He. *Phys. Rev. Lett.* **38**, 551 (1977).
55 K. W. Schwarz, Three-dimensional vortex dynamics in superfluid 4He. Homogeneous superfluid turbulence. *Phys. Rev. B* **38**, 2398 (1988).
56 J. T. Tough, "Superfluid turbulence" in *Progress in Low Temperature Physics*, D. F. Brewer, Ed. (North-Holland, 1982), vol. VIII, chap. 3.
57 J. Gao, E. Varga, W. Guo, W. F. Vinen, Energy spectrum of thermal counterflow turbulence in superfluid helium-4. *Phys. Rev. B* **96**, 094511 (2017).
58 J. Gao *et al.*, Decay of counterflow turbulence in superfluid 4He. *JETP Lett.* **103**, 648 (2016).
59 J. Hosio *et al.*, Superfluid vortex front: Decoupling from the reference frame. *Phys. Rev. Lett.* **107**, 135302 (2011).
60 S. R. Stalp, J. J. Niemela, W. F. Vinen, R. J. Donnelly, Dissipation of grid turbulence in helium II. *Phys. Fluid.* **14**, 1377 (2002).
61 T. V. Chagovets, A. V. Gordeev, L. Skrbek, Effective kinematic viscosity of turbulent He II. *Phys. Rev. E* **76**, 027301 (2007).
62 S. Babuin, V. S. L'vov, A. Pomyalov, L. Skrbek, E. Varga, Coexistence and interplay of quantum and classical turbulence in superfluid 4He: Decay, velocity decoupling, and counterflow energy spectra. *Phys. Rev. B* **94**, 174504 (2016).
63 A. Gordeev, T. Chagovets, F. Soukup, L. Skrbek, Decay of counterflow turbulence in He II. *J. Low Temp. Phys.* **138**, 549 (2005).
64 E. Varga, L. Skrbek, Dynamics of the density of quantized vortex lines in counterflow turbulence: Experimental investigation. *Phys. Rev. B* **97**, 064507 (2018).
65 M. S. Babuin, M.Stammeier, E. Varga, M. Rotter, L. Skrbek, Quantum turbulence of bellows-driven 4He superflow: Steady state. *Phys. Rev. B* **86**, 134515 (2012).
66 S. Babuin, E. Varga, W. F. Vinen, L. Skrbek, Quantum turbulence of bellows-driven 4He superflow: Decay. *Phys. Rev. B* **92**, 184503 (2015).